

Surface-micromachined electrostatic microrelay

Ignaz Schiele *, Jörg Huber, Bernd Hillerich, Frank Kozlowski

Fraunhofer-Institute for Solid State Technology, Hansastraße 27d, D-80686, Munich, Germany

Abstract

Three variants of electrostatically driven microrelays are reported. These switches have a high off resistance like conventional mechanical relays, but are also characterized by a low power consumption ($< 10 \mu\text{W}$) and a very low switching time ($< 50 \mu\text{s}$). These microrelays consist of a cantilever beam, a fixed-fixed beam and a torsion beam with a double-contact configuration. Because of the complete fabrication by surface-micromachining technology, there is no need for a chip-bonding process. This paper reports on design considerations, device concept, fabrication and performance of the microrelay. © 1998 Elsevier Science S.A. All rights reserved

Keywords: Microrelays; Microswitches; Electrostatic relays; Surface-micromachined relays; RF switches

1. Introduction

Relay applications are almost unlimited wherever switching functions are needed in a circuit, system or product [1]. Therefore microrelays are one of the most promising future micromachined products. The distinctive qualities of mechanical relays are mainly the low contact resistance and the complete isolation between actuation circuit and contact circuit, which is higher by three orders of magnitude than the corresponding junction resistance of solid-state relays (SSRs). Micromechanical relays offer additional qualities that are usually associated with SSRs: a very low switching time ($< 50 \mu\text{s}$), high shock resistance ($> 5000G$) and a low power consumption ($< 10 \mu\text{W}$) due to electrostatic actuation.

The microrelays introduced in this paper are designed for small-signal applications from d.c. to HF (high frequency). To transfer HF signals with a wide frequency range by planar lines, strip conductors of approximately $400 \mu\text{m}$ width are necessary. At this micrometre scale only microswitches can bridge a disconnection of the otherwise homogeneous strip conductor.

First investigations to fabricate a miniaturized relay with micromachining process technologies were done by Petersen [2]. Another bulk-micromachined microrelay concept was published later [3]. The disadvantage of this device is that a backside etch process is necessary to structure the deflectable contact carrier. This wet anisotropic etch process is mostly

performed by using KOH solution, but due to the anisotropic etching the device requires a relatively large area and a wafer- or chip-bonding process is needed to provide the operational function. In addition, KOH is not CMOS-compatible. A microrelay that was fabricated with only frontside etch process steps was introduced by Drake et al. [4]. A backside etch process has been avoided, but a wafer- or chip-bonding process is still necessary.

Mercury-wetted contact relays are normally selected for applications requiring freedom from contact bounce. Such a mercury-contact microrelay is described in Ref. [5].

Magnetic microrelays and magnetostatic 8×8 matrix relay for use in communication systems are reported in Refs. [6,7]. However, the electromagnetic actuation principle shows no pull-in instability, which is always observed by electrostatically actuated MEMS devices. A snap closing of the contacts, which is a main requirement for a relay, is therefore only achieved by using permanent magnets. This increases the size of the microrelay. Additional disadvantages are the long switching time, in the range 1 to 5 ms, and the high power consumption up to 320 mW compared to electrostatic actuation, which is an important issue for applications in wireless telecommunication systems.

A surface-micromachined switch with electrostatic actuation was reported [8] which was capable of handling gigahertz frequencies, but the gap between the fixed contacts and the contacting bar was only $3 \mu\text{m}$. This causes a high capacitance between the open contacts, which adversely affects the HF suitability.

To increase the HF isolation we fabricated microrelays with gaps of some $10 \mu\text{m}$ between the contacts by utilizing

* Corresponding author. Tel.: +49 89 547 59195. Fax: +49 89 547 59100. E-mail: ischiele@ift.fhg.de

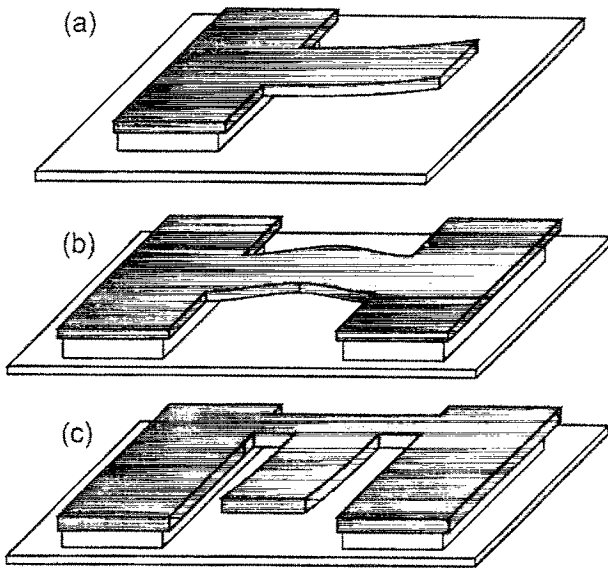


Fig. 1. (a) Cantilever beam, (b) fixed-fixed beam, (c) torsion beam.

the residual layer stresses. The microrelays are fabricated by surface micromachining, therefore, a wafer- or chip-bonding process is avoided. The area consumed by the microrelay is very small and the method is CMOS-compatible. The microrelay provides a bounce-free operation without the need for mercury-wetted contacts. In this paper we report on the device concept, theory, fabrication and device performance.

2. Device concept

To switch electric current or signals mechanically we use an electrostatically actuated moveable beam which carries the contacting bar. We designed three types of beams: a beam supported on one side (cantilever), a double-sided supported beam (fixed-fixed beam) and a torsion beam (Fig. 1).

With these configurations microrelays can be realized that are characterized by a small gap on the fixed end and a large gap at the contacting bar. The curvature of the beam is achieved by utilizing the residual stress in the beam, which

is a sandwich of $\text{SiO}_2\text{-Au-SiO}_2$ layers. The small gap between the deflectable beam and the bottom electrode is necessary to actuate the microrelay at a low operating voltage. The large gap between the contacting bar and the fixed contacts results in a relatively low capacitance between the contacts.

Additionally, an increased restoring force of the deflected beam is achieved. This high restoring force is necessary to reopen the switch, because the adhesive forces between the beam and the substrate and between the gold contacts have to be surmounted.

Fig. 2 shows a schematic view of the microrelay with double-contact configuration.

3. Theory

To calculate the pull-in voltage and to control the radius of curvature of the beams, it is important to know the value of the residual stress of the $\text{SiO}_2\text{-Au-SiO}_2$ sandwich layers. The residual stress is determined by measuring the bending of test structures. The following formulas are based on the assumption that the beams have only a pure bending. The residual stress σ_{xx} is given by

$$\sigma_{xx} = \frac{E}{1 - \nu^2} (\varepsilon_{xx} + \nu \varepsilon_{yy}) \quad (1)$$

where E is the effective Young's modulus of the beam material considering multiple layers, ν is the Poisson ratio, and ε_{xx} and ε_{yy} are the strain components. Because the stress is fairly uniform over the lateral plane we simplify:

$$\varepsilon = \varepsilon_{xx} = \varepsilon_{yy} \quad (2)$$

The strain component is calculated by

$$\varepsilon = \bar{\varepsilon}_{xx} + \kappa_x \frac{h}{2} \quad (3)$$

where $\bar{\varepsilon}_{xx}$ is the strain in the middle plane of the beam and κ_x is the curvature of the middle plane. Because the neutral axis

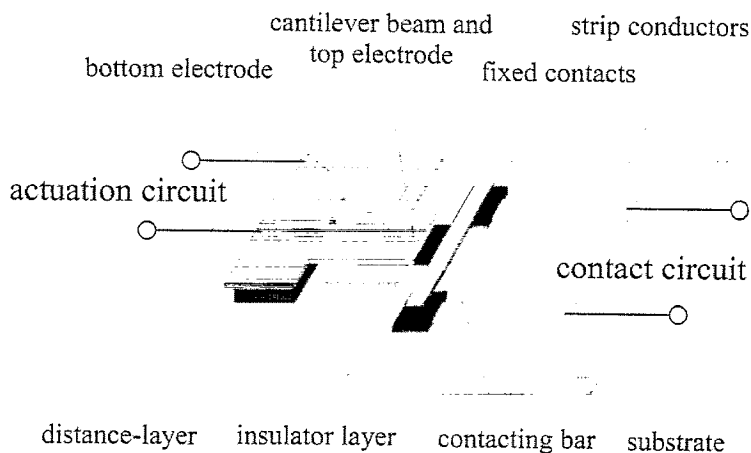


Fig. 2. Schematic view of the microrelay.

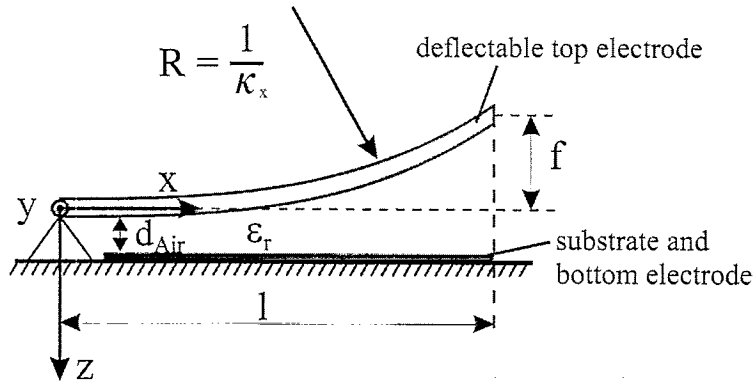


Fig. 3. Schematic illustration of the deflection of a curved beam.

passes through the centroid for rectangular sections, the neutral axis of the beam is located in the geometric centre at $z=0$. Therefore the maximum strain appears at the edge of the beam, which is located at $z=h/2$, where h is the thickness of the beam. The maximum strain is expressed in Eq. (3).

The actual curvature, κ_x , can be determined by measuring the deflection of the beam tip, f (see Fig. 3), and using the well-known curvature–deflection relation:

$$\kappa_x = 2f/l^2 \quad (4)$$

The strain term for cantilever beams can be calculated by setting $\bar{\epsilon}_{xx}=0$, where l is the length of the beam.

For fixed–fixed beams the strain term can be expressed by the change of the beam length. After releasing the structure a deformation takes place due to the residual layer stress. Because the beam is clamped at both ends, the bending causes a lengthening Δl of the beam. The strain is given by

$$\epsilon = \Delta l/l \quad (5)$$

The deflectable beams consist of three layers of different materials. The central layer is gold ($E_{Au}=57$ GPa); the top and bottom layers are made of an SiO_2 insulator layer ($E_{in}=64$ GPa); and the adhesion layer between Au and the SiO_2 layers is made of NiCr ($E_{ad}=110$ GPa). Such composed beams can be treated by using an equivalent width technique to calculate an effective modulus of elasticity E [9]:

$$E = E_{Au} \times \frac{\frac{bh_{Au}^3}{12} + 2 \left[\frac{E_{ad}bh_{ad}^3}{E_{Au}} + \frac{E_{ad}bh_{ad}}{E_{Au}} \left(\frac{h_{Au}}{2} + \frac{h_{ad}}{2} \right)^2 \right] + 2 \left[\frac{E_{in}bh_{in}^3}{E_{Au}} + \frac{E_{in}bh_{in}}{E_{Au}} \left(\frac{h_{Au}}{2} + h_{ad} + \frac{h_{in}}{2} \right)^2 \right]}{\frac{b}{12}(h_{Au} + 2h_{ad} + 2h_{in})^3} \quad (6)$$

E_i are the moduli of elasticity of the components, h_i are the thicknesses of the components and b is the width of the beam. The residual stress σ_{xx} of the composed beam at room temperature is therefore +65 MPa tensile stress.

A voltage V applied between the substrate and the metalization of the deflectable beam causes an electrostatic force (Fig. 3). Because of the etch access holes and the large cur-

vature of the beams, the fringing fields that are created on the edges of the beam have to be considered. But simulation of the capacitance of the perforated beam showed that the fringing fields almost compensate the reduction of the electric field due to the holes. To calculate the value of the electrostatic forces we assume for simplicity that the fringing fields and the etch access holes can be neglected. With these simplifications we get the electrostatic force F_E :

$$F_E(w, V) = \frac{1}{2} \epsilon_r \epsilon_0 b V^2 \int_0^l \frac{1}{(d - w(x))^2} dx \quad (7)$$

where b is the width and l the length of the beam, ϵ_0 is the dielectric constant of vacuum, ϵ_r is the dielectric constant of the gap medium and d is given by

$$d = d_{Air} + \frac{h_{SiO_2}}{\epsilon_{SiO_2}} \quad (8)$$

where d_{Air} is the gap of the fixed end, h_{SiO_2} is the layer thickness of SiO_2 and ϵ_{SiO_2} is the dielectric constant of SiO_2 . The deflection curve $w(x)$ of the beam due to residual stress is calculated by [10]

$$w(x) = \frac{f}{3} \left[3 - 4 \frac{l-x}{l} + \left(\frac{l-x}{l} \right)^4 \right] \quad (9)$$

In order to cause any displacement of the beam, the electrostatic force F_E must be larger than the restoring force F_R . The restoring force is the superposition of three components: (a) the bending of the beam along the x -axis due to residual stress; (b) the transverse bending of the beam along the y -axis due to residual stress; (c) the bending of the beam due to electrostatic force, with the assumption that the plane of the beam is horizontal and the deformation starts from this state.

The restoring force is given by

$$F_R(w) = F_{(a)} + F_{(b)} + F_{(c)} = \frac{\sigma_{xx} I_{yy}}{hl/2} + 2B(1-\nu) \left(\frac{2q}{l^2} + \frac{2q}{(b/2)^2} \right) + \frac{bh^3 E}{4l^3} w \quad (10)$$

where I_{yy} is the moment of inertia, w is the vertical deflection of the beam and q is the deflection of the outer beam tip

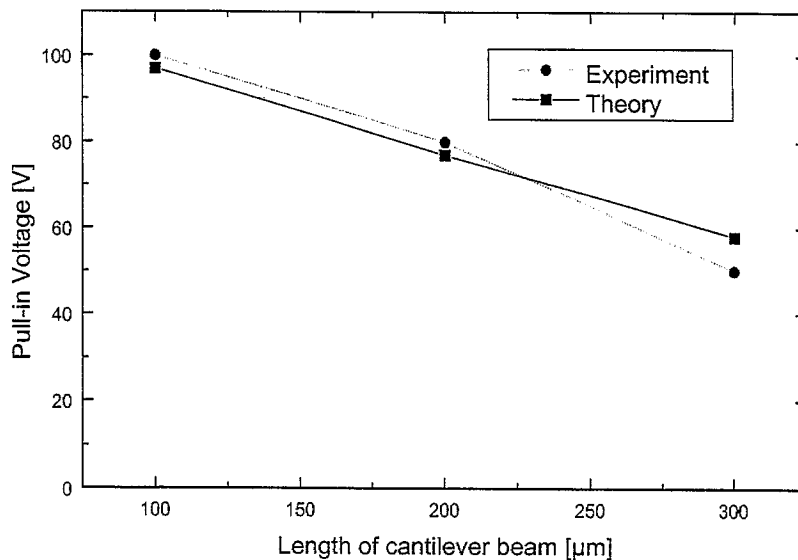


Fig. 4. Pull-in voltage of cantilever beams (beam width = 100 μm).

compared with the deflection of the beam tip in the central axis. Measurements showed that q is in the range 0.5–5 μm and B is

$$B = \frac{Eh^3}{12(1-\nu^2)} \quad (11)$$

The pull-in voltage V_{pi} is derived by setting

$$F_R(w) + F_E(w, V)_{V=V_{pi}} = 0 \quad (12)$$

The equation can be calculated numerically or graphically. Fig. 4 shows the relatively good agreement between experiment and theory. The investigations were done on a cantilever beam with a width $b = 100$ μm and $q = 1$ μm. The layer thicknesses are $h_{Au} = 200$ nm, $h_{ad} = 35$ nm and $h_{in} = 500$ nm.

4. Electrical contacts

The electrical contacts are crucial for the performance of such a device. Relay characteristics such as contact resistance and stability are strongly influenced by the quality of the contacts [11]. All electrical contacts should also have reasonable noise performance and good erosion characteristics for a given application [12]. Because a microrelay works with an ultra low contact force in the micronewton range and because only a little current capability is demanded, we use gold as the contact material. Gold is distinguished by a low and consistent contact resistance and inhibits the formation of alien films on the contact surfaces. It is well known that gold contacts tend to stick or to weld, therefore, an adequate contact breakaway force must be provided. This breakaway force is achieved by the high restoring force of the beams due to the curvature.

5. Fabrication

A four-mask fabrication process has been developed without the need for chip bonding. Fig. 5 is a schematic illustration of the process sequence. The fabrication starts with a silicon wafer. Because it is a surface-micromachining process, we are independent of the substrate material. So the silicon wafer could easily be replaced by a glass wafer or a ceramic sub-

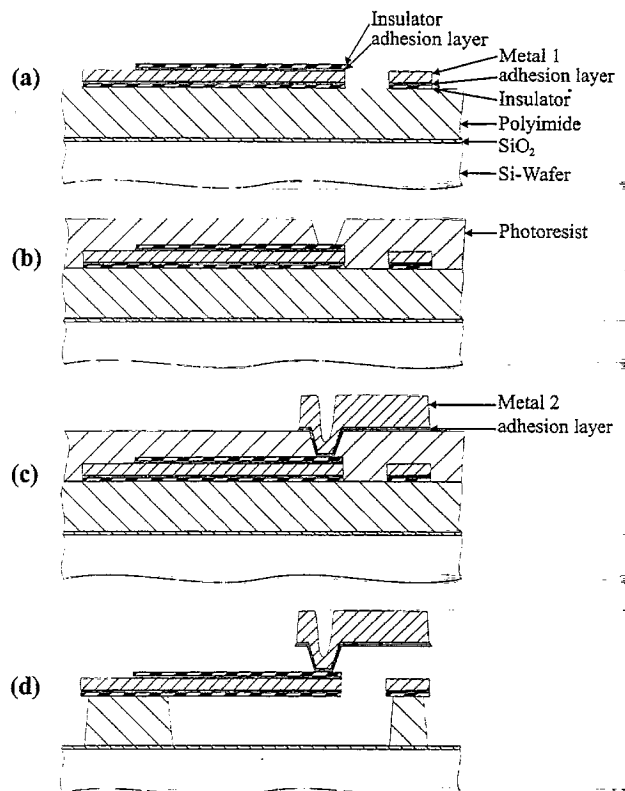


Fig. 5. Microrelay fabrication process.

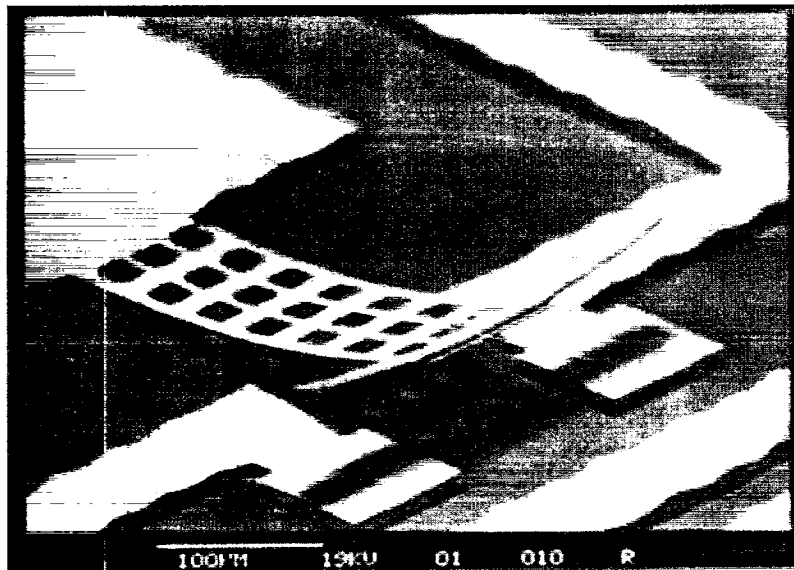


Fig. 6. Microrelay with cantilever beam.

strate. The first step is a dry thermal oxidation to obtain an SiO_2 layer. Next a $4\text{ }\mu\text{m}$ thick polyimide sacrificial layer is spun on, which can be removed in an oxygen plasma. Due to this dry etching process sticking problems can be avoided.

To prevent short circuiting between the beam and the bottom electrode, a dielectric layer is deposited. Next an adhesion layer, a metallization and the second adhesion layer are deposited. To separate the actuation circuit and the signal circuit electrically, a second insulation layer is necessary. After patterning of the composed beams, the bondpads and the contact pads are opened (Fig. 5(a)). Now a second sacrificial layer is necessary to form the contact bars (Fig. 5(b)). After exposure of the photoresist, gold (Au) is electroplated. The contact bars are patterned by a dry etch process (Fig. 5(c)).

The sacrificial layers are etched for 3.5 h in an oxygen plasma-etching process. This only frees the beams and bridges, but keeps the anchor pads still attached to the substrate (Fig. 5(d)). The final result is shown in Fig. 6.

6. Device performance

To operate the cantilever beams, a pull-in voltage from 20 to 100 V was necessary. Short cantilever beams require a higher voltage than longer beams. Narrow beams ($b=50\text{ }\mu\text{m}$) are activated by a lower pull-in voltage than wider beams ($b=100\text{ }\mu\text{m}$) due to the reduced transverse bending. Because of the high restoring force of the beams due to the curvature, the sticking phenomenon can be avoided. The switching performance is therefore reliable and stable.

To calculate the shock resistance the spring constant c of the beam was extracted from the measured hysteresis (Fig. 7). With a release voltage of 20 V and an adhesion energy of 0.04 J m^{-2} [13] for silicon surfaces, a spring constant $c=45\text{ N m}^{-1}$ results from the equilibrium of adhe-

sion force plus electrostatic force and the restoring force of the beam. Because of the very lightweight cantilever beam (mass = $0.5\text{ }\mu\text{g}$) a theoretical shock resistance of $10^5 G$ is expected.

The lowest required actuation voltage for cantilever beams is 20 V with an actuation current caused by leakage of 50 nA. Thus the power consumption is $1.0\text{ }\mu\text{W}$.

With a four-point probe measurement various test devices with widths varying from 50 to $200\text{ }\mu\text{m}$ and lengths from 100 to $300\text{ }\mu\text{m}$ have been investigated. For these different microrelays contact resistances of 10 to $80\text{ }\Omega$ were observed. The contact resistance is a function of the contact pressure, which varies with the value of the actuation voltage and with the contact area. This might be the reason for the spread of the contact resistance.

A long-term reliability test of the microrelay was performed using a computer-controlled actuation and measurement set-up. The contact resistance is measured and recorded after each operation. During the device test the microrelay was unprotected from dust or other disturbances in the surrounding air. The current load was 1 mA. Fig. 8 shows the typical on-resistance of a microrelay. In the first part of the operation cycles a high scatter and value of the contact resistance is observed. A few contacts failed completely ($R > 200\text{ }\Omega$) due to contamination on the contact surfaces. After about 200 cycles the alien films are burned away and the contacts show a consistent contact resistance typical for the gold contact material. The cantilever microrelay has a mechanical lifetime of over a million cycles (with no contact load) and a electrical lifetime (with contact load) of over 7000 cycles.

Fig. 9 shows the dynamic contact performance of a cantilever microrelay. After applying the pull-in voltage, a switching time of only $2.6\text{ }\mu\text{s}$ is required to close the contacts. The time required for closing the contacts depends on the mass of the moving part and on the distance between the contacts. The gap between the contacting bar and the fixed contacts is

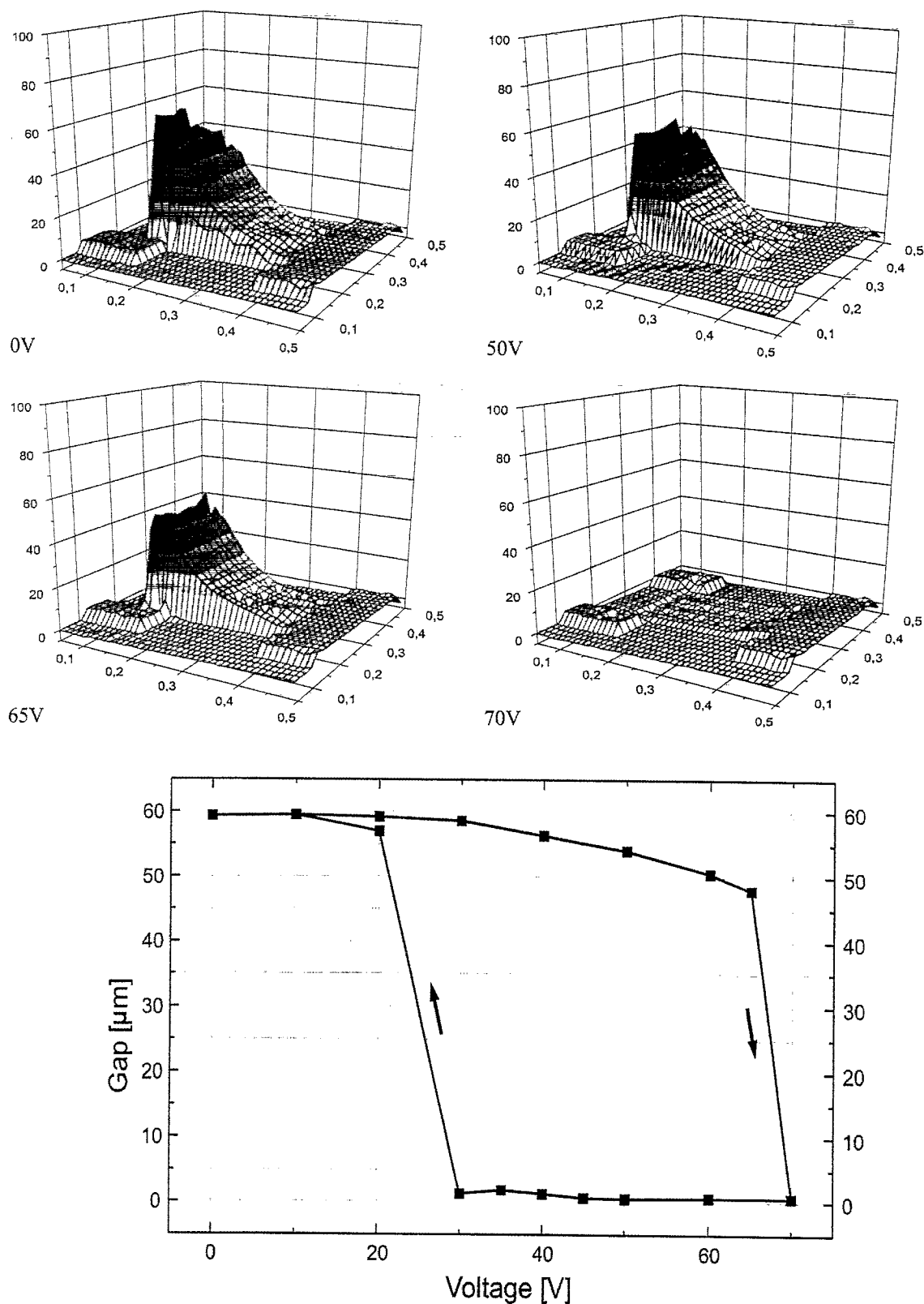


Fig. 7. Switching sequence and gap vs. voltage of a cantilever microrelay.

10 μm for the cantilever beams of 100 μm length. For longer beams ($l=300\text{ }\mu\text{m}$) the gap amounts to 60 μm. The corresponding switching time is 20 μs.

The bounce-free operation is provided by the absorption of the kinetic energy of the moving parts at the instant of impact. But not only the flexibility of the contacting bar and

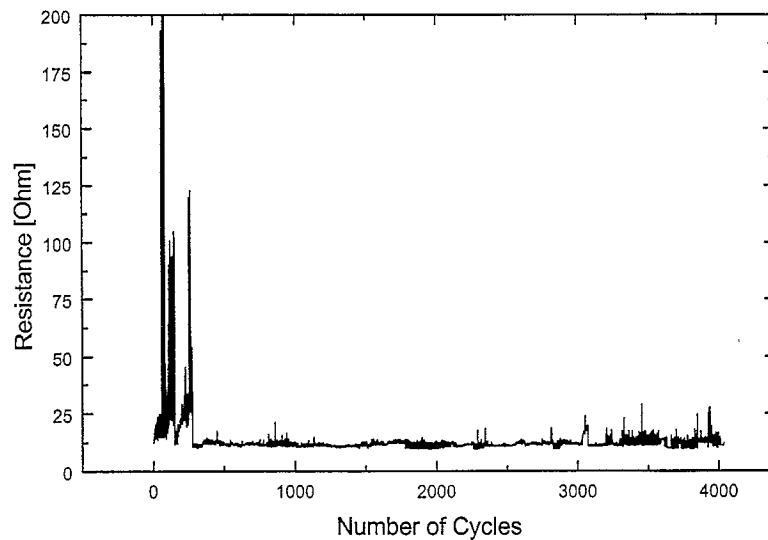


Fig. 8. On-resistance of microrelay.

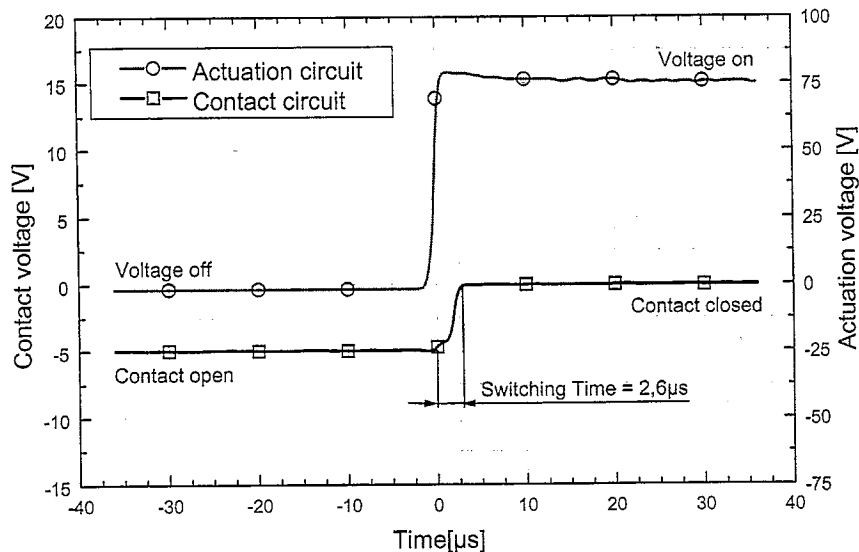


Fig. 9. Time trace of cantilever microrelay.

the cantilever beam prevent contact bounce; the freedom from contact bounce is also supported by the increase of the electrostatic force (for a decrease of the distance between the electrodes), which keep the contacts closed.

The required pull-in voltage for fixed–fixed beams is higher than for cantilever beams (between 60 and 150 V), but also an increased restoring force is achieved. This is the reason why sticking failure of the double-clamped microrelays during operation is very unlikely.

Because of the residual stress of the thin films, the beams are stretched. This strain causes a deformation of the fixed–fixed beams (Fig. 10(a)). The freestanding structure of the fixed–fixed beam is therefore longer than the distance between the fixed ends. When the pull-in voltage is applied, the beam descends and the signal circuit is closed (Fig. 10(b)).

The gap spacing of the microbridges varies from 30 to 70 μm , so a longer switching time (25 μs) is necessary to close

the contacts. An increase in kinetic energy results from higher speed of the contacting bar when it strikes the fixed contacts. The moving structures of fixed–fixed beams do not have sufficient kinetic energy to cause mechanical rebound, but a chatter or 'dynamic resistance' due to a variation in contact pressure is observed (Fig. 11).

The third variant investigated was a device which was expected to rotate about a torsion beam (Fig. 12). Due to intrinsic stress, however, the torsion beam buckled and the switching behaviour was bistable. The overall performance was poor.

In terms of reliability, the cantilever beam and the fixed–fixed beam are much better than the torsion beam. With respect to the required pull-in voltage the cantilever beam is the best. However, if a high restoring force is needed, a fixed–fixed beam seems better.

The characteristics of the three types of microrelays are listed in Table 1.

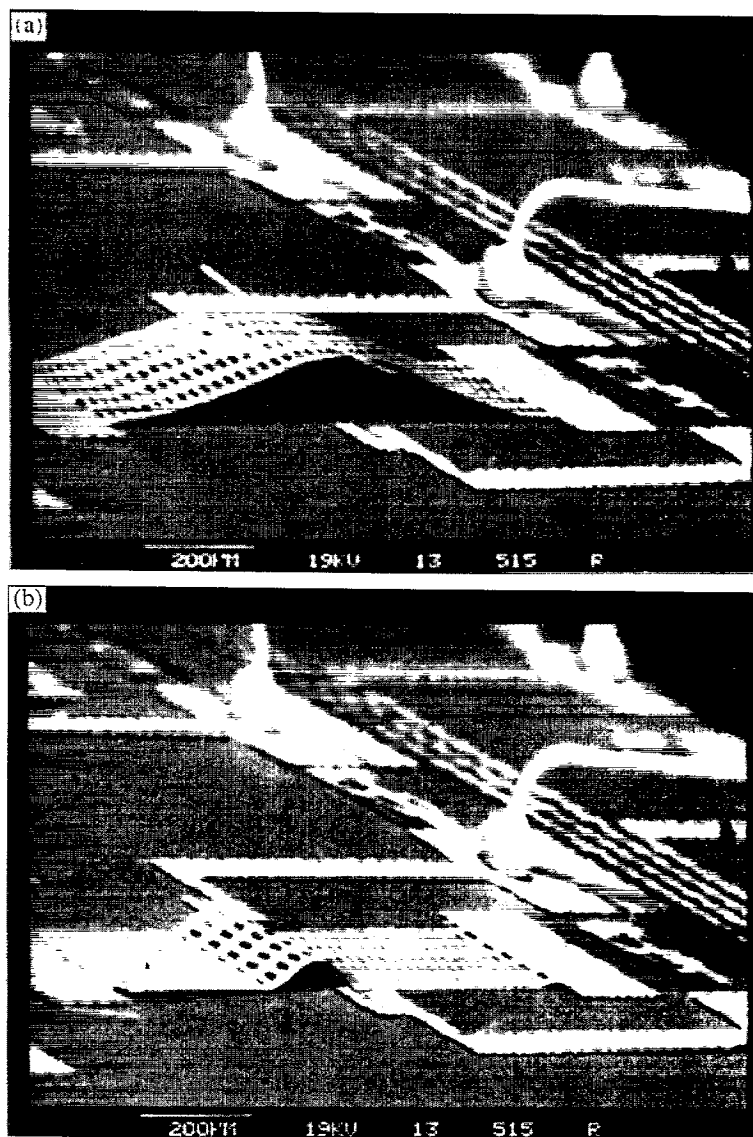


Fig. 10. Fixed-fixed beam relay (a) open and (b) closed.

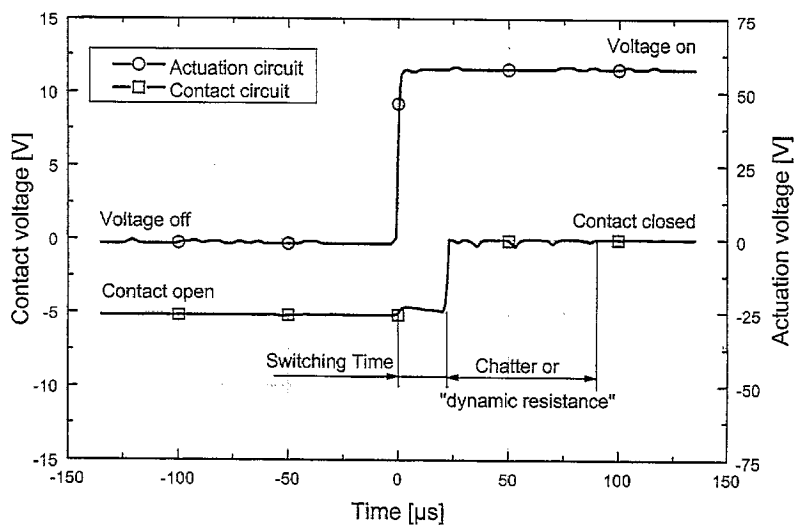


Fig. 11. Time trace of fixed-fixed beam.

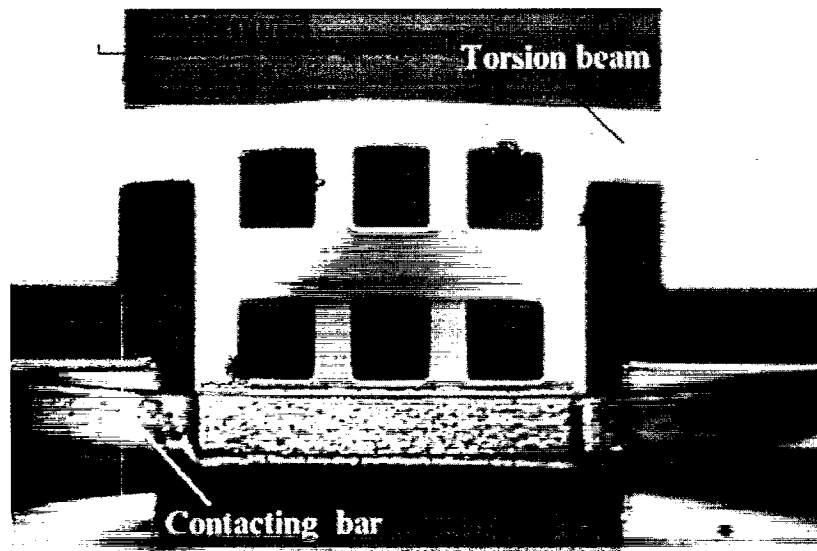


Fig. 12. Torsion beam.

Table 1
Results for different types of microrelays

Geometry	Cantilever beam	Fixed-fixed beam	Torsion beam
Pull-in voltage	20–100 V	60–150 V	150 V
Actuation current	50 nA	70 nA	60 nA
Power consumption	1.0–4.5 μ W	4.2–10.5 μ W	9 μ W
Switching time	2.6–20 μ s	14–45 μ s	24–33 μ s
Current capability	1 mA	1 mA	1 mA
Contact resistance	10–80 Ω	15–80 Ω	15–60 Ω
Area consumption (excluding bondpads)	0.03–0.1 mm ²	0.2–0.7 mm ²	0.04 mm ²

7. Conclusions

A pull-in voltage model of cantilever microrelays has been presented. A good agreement with measured pull-in voltages was achieved, because the bending of the cantilever beam along the length direction and along the width direction was taken into account.

Several types and various test devices of microrelays have been fabricated in a four-mask process. The microrelays are actuated electrostatically, therefore, a snap closing of the contacts is achieved.

With cantilever beams a switching time of 2.6 μ s was measured. Including bondpads, this type of device covers an area less than 1 mm². The small area consumption is achieved by a surface-micromachining fabrication process.

To avoid the sticking problem, fixed–fixed beams were also fabricated. An increased restoring force is provided by this type of microrelay, but also a higher pull-in voltage was necessary.

The performance of the torsion beams was poor due to the snapping motion.

Contact resistance was measured and recorded after each cycle with a computer-controlled probe station. The measurements have shown a contact resistance at 10 Ω . It has been demonstrated that the microrelay has at present a mechanical

lifetime of over a million cycles (with no contact load) and an electrical lifetime (with contact load) of over 7000 cycles. Measurements have shown that a mechanical switching frequency up to 3 kHz is possible.

Further work is under way to increase the lifetime and to reduce the contact resistance of the microrelay.

Acknowledgements

The authors wish to thank S. Vogel, U. Schaber and K. Kühl for their efforts in fabricating the device. We would also like to thank W. Hohenester, K. Beister and R. Jünemann from Rohde and Schwarz for helpful discussions.

References

- [1] Engineers' Relay Handbook, National Association of Relay Manufacturers, Milwaukee, WI, USA, 1996, p. 2-1.
- [2] K.E. Petersen, Micromechanical membrane switches on silicon, IBM J. Res. Develop., 23 (1979) 376–385.
- [3] H. Schlaak, F. Arndt, M. Hanke and J. Schimkat, Silicon-microrelay with electrostatic moving wedge actuator — new functions and miniaturisation by micromechanics, Micro System Technologies 96, Potsdam, Germany, 1996, pp. 463–468.

- [4] J. Drake, H. Jerman, B. Lutze and M. Stuber, An electrostatically actuated micro-relay, Tech. Digest, 8th Int. Conf. Solid-State Sensors and Actuators (Transducers '95/Eurosensors IX), Stockholm, Sweden, 25–29 June, 1995, pp. 380–383.
- [5] J. Simon, S. Saffer, C.-J. Kim, Mercury-contact switching with gap-closing microcantilever, Proc. SPIE, Vol. 2882, 14–15 Oct., 1996, Austin, TX, USA, 1996, pp. 204–209.
- [6] W.P. Taylor and M.G. Allen, Integrated magnetic microrelays: normally open, normally closed, and multi-pole devices, 9th Int. Conf. Solid-State Sensors and Actuators (Transducers '97), Chicago, USA, 16–19 June, 1997, pp. 1149–1152.
- [7] H. Hosaka and H. Kuwano, Design and fabrication of miniature relay matrix and investigation of electromechanical interference in multi-actuator systems, MEMS '94, Oiso, Japan, 1994, pp. 313–318.
- [8] J.J. Yao and M.F. Chang, A surface micromachined miniature switch for telecommunications applications with signal frequencies from DC up to 4 GHz, Tech. Digest, 8th Int. Conf. Solid-State Sensors and Actuators (Transducers '95/Eurosensors IX), Stockholm, Sweden, 25–29 June, 1995, pp. 384–387.
- [9] W.C. Young, Roark's Formulas for Stress and Strain, McGraw-Hill, New York, 6th edn., 1989, pp. 117–118.
- [10] Dubbel, Taschenbuch für den Maschinenbau, Springer, Berlin, 17th edn., 1990, C20.
- [11] H. Ziad, K. Baert and H.A.C. Tilmans, Design considerations of the electrical contacts in (micro)relays, Proc. SPIE, Micromachined Devices and Components II, Austin, TX, USA, 1996, pp. 210–217.
- [12] S.P. Sharma, Adhesion of electrical contacts, Proc. 3rd Int.–22nd Annual National Relay Conf., Stillwater, OK, USA, 1974, pp. 1–1–14.
- [13] M. Biebl, Physikalische Grundlagen zur Integration von Mikro-mechanik, Sensorik und Elektronik, Dissertation, Universität Regensburg, 1995.

Biographies

Ignaz Schiele received the Diploma in mechanical engineering from the Technical University of Munich in 1995. In his graduate work, he developed a surface-micromachined microrelay that was fundamental for the presented state. Currently he continues research work on the microrelay and is part of the MEMS design and layout group at the Fraunhofer-Institute for Solid State Technology, Munich, Germany.

Jörg Huber was very helpful in measurements of the micro-relay. He has now joined Siemens AG for further education.

Bernd Hillerich received the Diploma in physics from the University of Bonn in 1974 and the Ph.D. in electrical engineering from the Technical University of Berlin, Germany, in 1987. From 1975 to 1979 he was with AEG-Cable, Mülheim, to develop optical-fibre cables and measuring methods. Subsequently, at Philips Communications Industrie, Cologne, Germany, he developed measuring equipment, e.g., OTDRs, for optical-fibre links. In 1981 he joined AEG Research Centre, Ulm. He was engaged in research and development projects in various fields of optics, optoelectronics and communication, e.g., integrated optics, silicon micro-machining, processing of fibre-optical components, analog and digital transmission systems, microoptic and optoelectronic hybrids and optical amplifiers. In 1993 he became head of product development of the Sensor Division of Weidmueller Interface, Gaggenau, who produced sensor systems for laser material processing. In the successor company, Precitec GmbH, he was responsible for development and production. In 1995 he transferred to Quarzkeramik GmbH, Stockdorf (near Munich) and led the R&D department which was engaged in crystal oscillators and quartz resonator technology. Since October 1995 he has been with the Fraunhofer-Institute for Solid State Technology and heads the MEMS Department. Dr Hillerich has authored or coauthored about 60 technical papers and is a member of the IEEE.

Frank Kozłowski is a researcher at the Fraunhofer-Institute for Solid State Technology, where he manages the Physical Sensor Group. He is working on the development and improvement of micromechanical systems. In 1991 he received his Diploma degree in physics and in 1997 his doctorate from the Technical University of Munich with work about electroluminescent porous silicon.